A New Multimodal Biometric System Based on Finger Vein and Hand Vein Recognition

Randa Boukhris Trabelsi[#1], Alima Damak Masmoudi[#2], and Dorra Sellami Masmoudi[#3]

[#]Computer Imaging and Electronics Systems group (CIELS) from Control and Energy Management Laboratory(CEM-Lab), Sfax Engineering School, Tunisia, BP W, 3038 Sfax, Tunisia, Phone: (216-74) 274.088, Fax. (216-74)275.595.

[1] trabelsiboukhrisranda@live.fr [2]damak_alima@yahoo.fr [3]dorra.masmoudi@enis.rnu.tn

***Abstract*—As a reliable and robust biological characteristic, the vein pattern increases more and more the progress in biometric researches. Generally, it was shown that single biometric modality recognition is not able to meet high performances. In this paper, we propose a new multimodal biometric system based on fusion of both hand vein and finger vein modalities. For finger vein recognition, we employ the Monogenic Local Binary Pattern (MLBP), and for hand vein recognition an Improved Gaussian Matched Filter (IGMF). Experimental results confirm that the proposed multimodal biometric process achieves excellent recognition performance compared to unimodal biometric system. The Area Under Curve (AUC) of the proposed approach is very close to unity (0.98).**

Keywords-Multimodal Biometric System, Finger Vein, Hand Vein, MLBP, IGMF, ANN, Score Level Fusion.

I. INTRODUCTION

Biometric identification system based on physiological traits includes finger print[1], [2], palm print[3], [4], face [5],...etc. largely used in security applications Those modalities present considerable results. However, unimodal biometric systems present some limitations such as:

- Noise in captured data.
- Intra-class variations and inter-class similarities.
- Non-universality.
- Inter-operability issues.
- Spoof attack performance and fraud.

Accordingly, multimodal biometric systems are expected to be more reliable and they attract more research interests [6], [7], [8], [9]. The complex vascular pattern present inside the hand or finger potentially allows the computation of a good set of features that can be used for personal identification. This is the mean idea behind the proposition of a new human identification based on hand vein and finger vein modalities. Various features for identification of biometric system have been mentioned in the literature. Best results are always achieved by the multimodal systems and mainly for systems based on vascular characteristic.

Table I shows the relation between the characteristics for recognition in terms of performance (EER: Equal Error Rate, FRR: False Rejection Rate and FAR: False Acceptance Rate). The results in Table I are obtained by the multimodal biometric system based on two modalities.

TABLE I
Related survey systems example.

Year	Biometric system	Users	Experimental Results
Kumar et al [10]	hand geometry and Palmprint	100	FAR=0; FRR=1.41
Kumar et al [11]	knuckle shape and Vascular structure	100	EER=1.14
kang et al [12]	Geometry of the finger and Vascular structure	102	EER=0.075
GiTae et al [8]	geometry of the hand and vascular structure	100	EER=0.06

In this paper, we propose a multimodal biometric system integrating hand vein and finger vein modalities. Our multimodal biometric system has the advantage of having a single sensor to acquire two biometric traits with low cost. We perform the proposed multimodal system by a score-level fusion after normalization. Experimental results prove an improvement recognition performance compared to others systems.

This paper is described as follows: In section II, we describe the recognition process of finger vein and hand vein characteristics. In section III, a multimodal biometric system is presented and a fusion performed at

score level. Finally, in section IV, we present and discuss the experimental results followed by a conclusion.

II. PROCESS OF BIOMETRIC SYSTEM

The process of biometric system involves: image acquisition, preprocessing, feature extraction and classification.

A. Image Acquisition System

1) Finger Vein Database: Finger vein postures were taken from the available SDUMLA-HMT database [13]. This database includes a multimodal data (face, finger vein, iris, finger print and gait) from 106 individuals. The SDUMLA-HMT is the first available open access database. The acquisition system is conceived by Joint Lab of Wuhan University for Intelligent Computing and Intelligent Systems. Each subject contains his/her code as index, middle and ring finger of both hands. The set of 6 fingers is repeated 6 times to obtain 6 finger vein images. Accordingly, finger vein database includes 3,816 images. All images are encoded in "bmp" format by a resolution of (320 × 240). At the end, finger vein database takes up around 0.85 GBytes approximately. In Fig. 1, we present an example of postures from finger vein database.

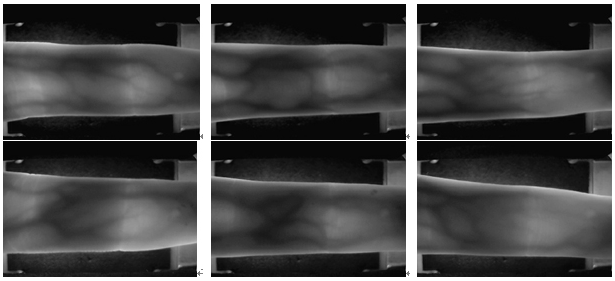

Fig. 1. Example of postures from finger vein database.

2) Hand Vein Database: Hand Vein images are taken from the Bosphorus Hand Database [14]. Images from this database are taken using a NIR technology using with monochrome NIR CCD camera (WAT-902H2 ULTIMATE). All images are encoded on 8 bits and have size of (300 × 240) with a "bmp" format. Furthermore, hand vein images are taken under normal and different conditions such as:

- Images taken under normal condition are referred to as (norm)
- Images taken after under taking an activity are referred to as (act).
- Images taken after carring a bag weighting 3 kg are referred to as(bag).
- Images after having cooled the hand by holding an ice pack on the back of the hand are referred to as (ice).
- Images after a time lapse ranging from two months to five months referred to as (timelapse).

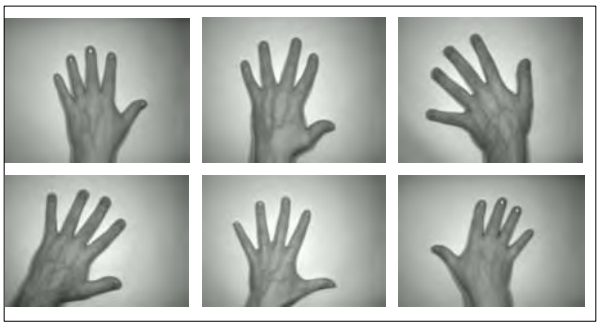

Fig. 2. Samples of hand vein images.

B. Preprocessing System

In biometric identification process, preprocessing module is necessary to ensure denoising, enhancement contrast and extract the Region of Interest(ROI). Since hand vein and finger vein present approximately a same visibility and structure, we use a same denoising and enhancement contrast in the preprocessing block. This latter, is described in the following.

1) ROI Extraction:

- ROI of finger vein:

Mathematical morphology operator is investigated in mathematics and geometry theory [15]. The operation technique is a variant of the morphological mathematic operator. This method makes the object contour

smoother and disconnects the narrow gap and eliminates fine prominence [16]. Then, Hough transform technique is applied for edges extraction. In Fig. 3, we illustrate the ROI region with respect to finger vein.

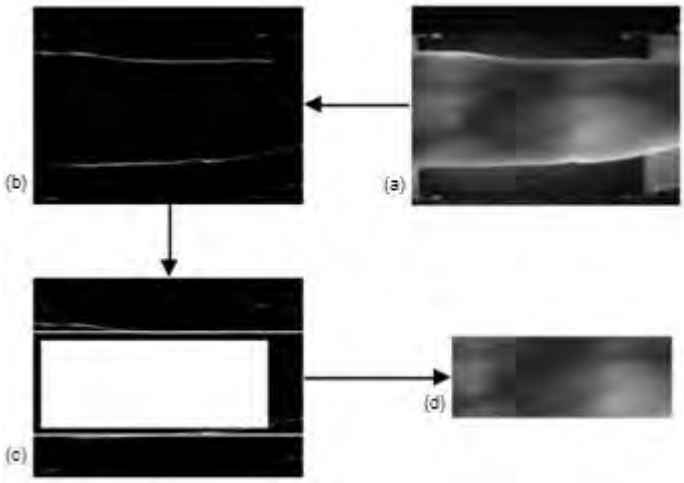

Fig. 3. Preprocessing steps: (a) Original image, (b) Fingervein contour image, (c) ROI mask based on the fingervein contour, (d) ROI image.

- ROI of hand vein:

The center of the hand vein image is extracted as the ROI center. The proposed algorithm of ROI extraction of hand vein image includes five steps:

– A hand vein binary image is obtained by a simple threshold based on Otsu method.

– Boundaries from the binary image are detected by canny operator.

– Valleys of hand between index and middle fingers and betwen little and ring fingers are detected.

– A geometrical technique is investigated to draw the line connecting the two keys points determined in the previous step and the line perpendicular to it.

– A sub-image is detected and extracted as the ROI of hand vein image. An original image and the ROI extracted from it are illustrated in Fig. 4.

2) Image denoising: The median filter is applied to the original hand and finger vein image for denoising. Then, a 2D Wiener filter is applied to remove the effect of high level frequency noise. The 2D Wiener filter has been implemented, assuming a "Gaussian white noise" is present in the vein image. The proposed denoising approach presents a less complexity and superior performance. A hand and finger vein prints are illustrated in Fig. 5 after the denoising step.

3) Vein Image Enhancement: The acquired hand or finger vein image presents generally a poor contrast and a dynamic illumination. To improve contrast and make emphasis on the discriminant details in the image, a Contrast Limited Adaptive Histogram Equalization (CLAHE) is proposed as a method to enhance vein image [17]. The CLAHE is an efficient method reorganizing the vein image and is suitable for improving local contrast underlying more details. Fig. 6 illustrates the enhanced contrast of a vein image.

C. Feature Extraction

1) Finger Vein Feature Extraction: Finger vein images obtained from the available database described in section (II-A1) can be characterized by texture pattern. So, to extract discriminant information of vein structure, we propose the use of texture descriptor. Indeed, Ojala et al provides a robust means to describe local binary patterns in texture [18]. Using the LBP operator, we will be (2^8 = 256) texture variants possible.

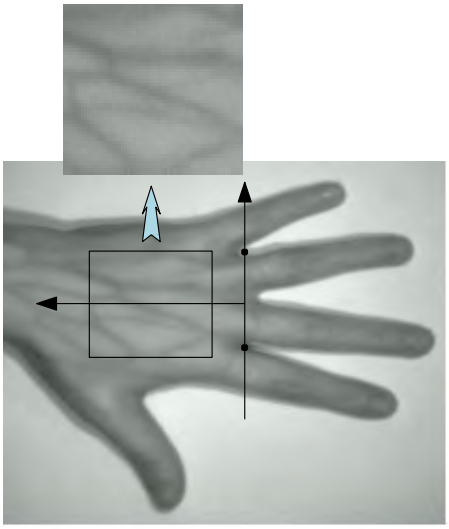

Fig. 4. ROI extraction from a hand vein image.

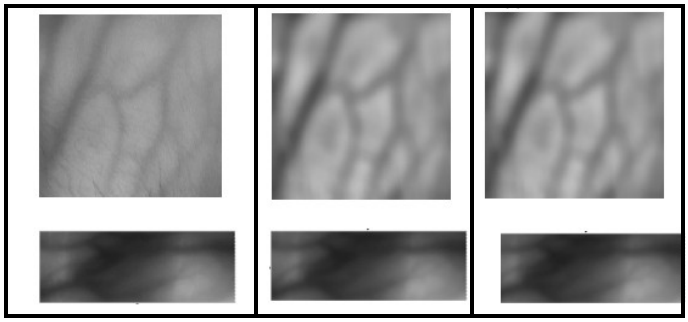

(a) (b) (c)

Fig. 5. Finger and hand vein prints after denoising: (a) ROI of vein image; (b) ROI after median filter application; (c) ROI after Wiener filter application.

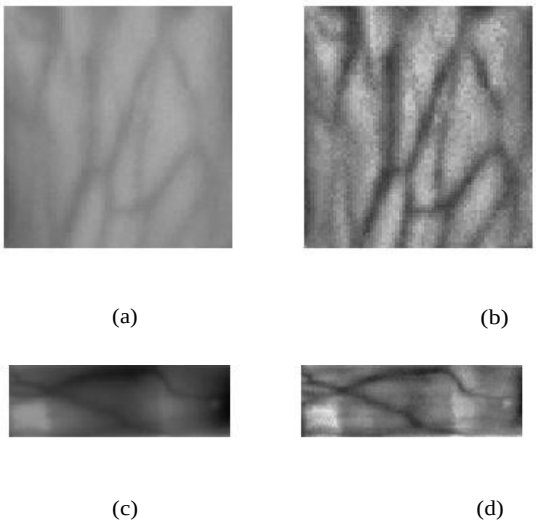

(a) (b)

(c) (d)

Fig. 6. Vein print image enhancement: (a) ROI of hand vein image; (b) Hand vein print processed by CLAHE; (c) ROI of finger vein image;(d) Finger vein print processed by CLAHE

For each pixel, a window of a (3 × 3) neighborhood is thresholded by the value of the central pixel. Therefore LBP code is defined by these relations:

$$LBP_{P,R} = \sum_{P=0}^{P-1} S(g_p - g_c)2^P \quad (1)$$

$$S(x) = \begin{cases} 1, & x > 0 \\ 0, & x < 0 \end{cases} \quad (2)$$

Where:

- g_C is the gray level value of the central pixel.
- g_P is the gray level value of its neighbors.
- P is the number of neighbors.
- R is the radius of the neighborhood.

Thus, if the coordinates of the central pixel g_c are $\{x_c = 0 \text{ and } y_c = 0\}$, the coordinates of g_p are defined by these equation:

$$\begin{cases} x_p = \frac{-R \sin(2\pi p)}{P} \\ y_P = \frac{R \cos(2\pi p)}{P} \end{cases} \quad (3)$$

As amelioration and to achieve invariance with the rotation of patterns, we can define the rotation invariant pattern by the following equation:

$$LBP_{P,R}^{riu2} = \begin{cases} \sum_{p=0}^{p-1} u(g_p - g_c) & if \ \ U(LBP_{P,R}) \le 2 \\ P+1 & otherwise \end{cases} \quad (4)$$

The Monogenic Local Binary Pattern (MLBP) includes the $LBP_{P,R}^{riu2}$, the local phase and the local surface with 1st-order and 2nd-order.

The local phase and the local surface are defined respectively as:

$$\varphi_c = \lceil \varphi/(\pi/M) \rceil \quad (5)$$

$$\zeta_c = \begin{cases} 0, & \det(T_c) \le 0 \\ 1, & otherwise \end{cases} \quad (6)$$

where $det(T_c)$ is the determinant of curative tensor. The image histogram MLBP response is the vector characteristic in the classification phase. In Fig. 7, we have shown an example of ROI of finger vein image and its correspondent histogram.

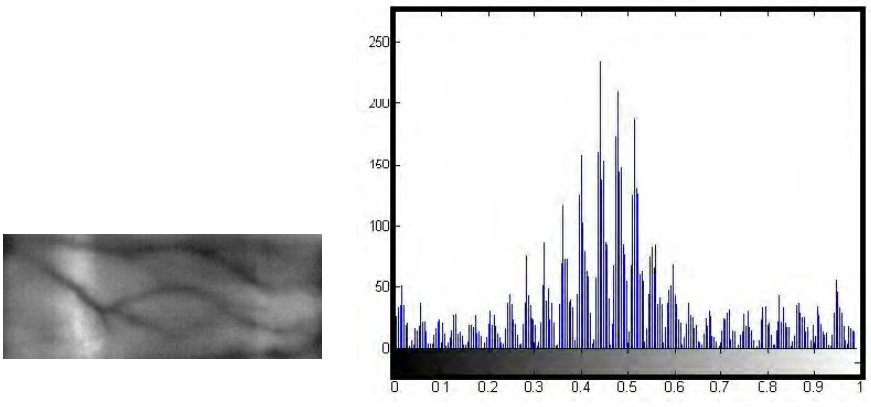

Fig. 7. ROI of Finger vein and its correspondent histogram issued from MLBP code.

2) Hand vein Feature extraction: The hand vein images collected in Phosphorus database have a good quality after denoising and enhancement contrast. Therefore, we propose here a simple method to extract vessels as features from hand vein images. We do not need to use a texture descriptor to improve the distribution of gray level because you can lose relevant information. The proposed method aims to introduce an improved Gaussian Matched Filter (GMF) [19] as a method to detect the vein of hand image. Typically, GMF is defined by equation (7).

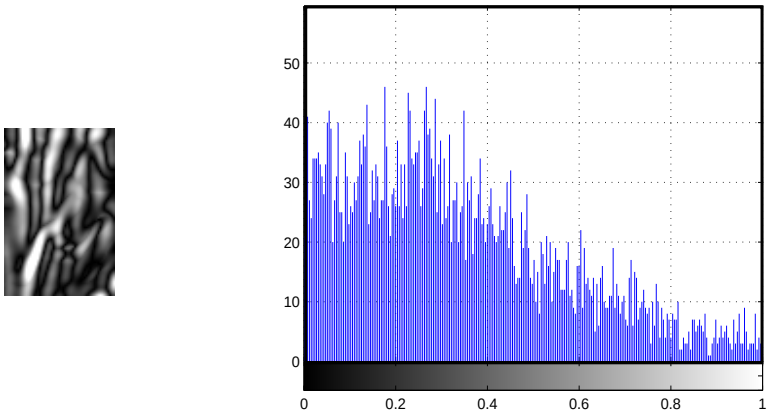

Fig. 8. Hand vein image obtained after the IGMF and its corresponding histogram.

$$f_\theta(x,y) = \frac{1}{\sqrt{2\pi}\sigma}\exp\left(-\frac{x'}{2\sigma^2}\right) - m,$$
$$|x'| \le 3s\,;\ |y'| \le \frac{L}{2}, \qquad (7)$$
$$x' = x \times \cos(\theta) + y \times \sin(\theta),$$
$$y' = y \times \cos(\theta) - x \times \sin(\theta).$$

where σ is a scale value of a kernel filter, with orientation θ mean value of m and with a length of neighborhood along *y*- axis *L*.

The response of the GMF is obtained by the 2D convolution between the kernel filter and the original image. To ensure that the response of the filter detects only vessels and not edges, we improve the GMF by its fusion with its first derivative as IGMF. The mean idea is to have two symmetrical responses to verify that's a true vessel. Besides, if the two responses are anti-symmetrical, we can verify that's a false vessel, identified to an edge or a noise in the image.

In the experimental study, we chose a window of size (3 × 3) composed by eight directions (0o; 45o; 90o; 135o; 180o; 225o; 270o; 315o). Fig. 8 gives an example of ROI of hand vein image after applying a IGMF filter and its corresponding histogram.

D. Classification with ANN

Typically, the Artificial Neural Networks (ANN) based classified technique is used for classification attributes. Each attribute based on finger vein and hand vein is classified with ANN after a fusion step is achieved. The ANN ensures the passage from the coding space to the decision space. The ANN is inspired from the biological nervous system.

Let $In = (In_1, In_2, ..., In_d)^T$ be an input of attribute vector and $W = (w_1, w_2, ..., w_d)^T$ the weight respective vector, the output out is presented as:

$$out = sig(w^T x_b) = g\sum_{i=1}^{d} w_i\, x_i - b \qquad (8)$$

where *sig(.)* is namely a sigmoidal activation function determined by equation (9). Fig. 9 shows the slope of this activation function. The applied network architecture is shown in Fig. 10.

$$sig(x) = (1 + exp^{-x})^{-1} \qquad (9)$$

The error of testing and learning phase is computed as follows:

$$E = \frac{\sum_{i=1}^{n}(out - T)}{N_b} \qquad (10)$$

where *out* is the output resulting from ANN output , *T* is the desired target and N_b is the number of the used samples. After training steps, generalization error was evaluated for different features and network conditions.

Fig. 11 shows the evolution of training and generalization errors by incrementing the number of hidden layers. From Fig. 11, we can see that the training error using just 5 neurons in the hidden layer does not exceed the value of 0.1% for training phase and 0.35% for testing phase.

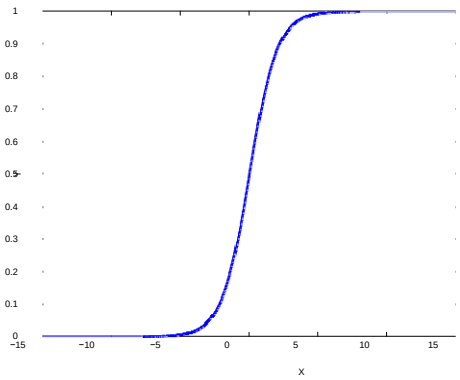

Fig. 9. The slope of sigmoidal activation function

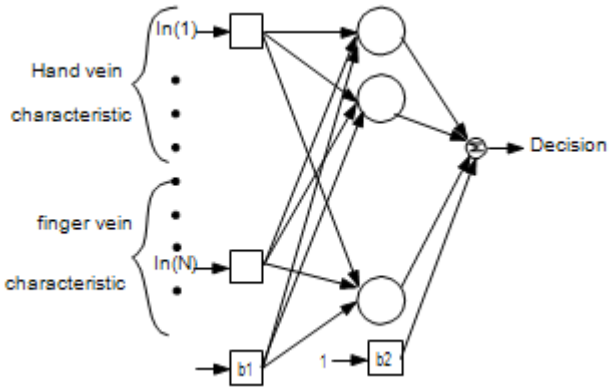

Fig. 10. The applied network.

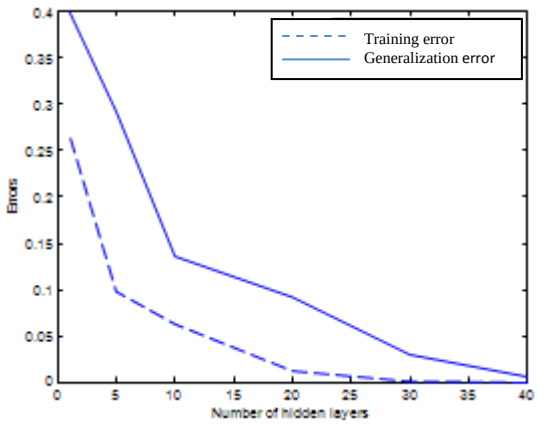

Fig. 11. Evolution of training and generalization errors by increasing the number of neurons in the hidden layers

III. MULTIMODAL SYSTEM

A. *Overview*

The overall architecture of the proposed multimodal biometric system is illustrated in Fig. 12. Hand vein identification or finger vein identification all involve image preprocessing, feature extraction, classification matching score and final decision.

B. *Score Level Fusion*

The Multimodal biometric system is generated by matching score levels issue from each characteristics. We achieve here the matching score level with a simple sum. First, we normalize the score into a same interval such [0 1]. This transformation

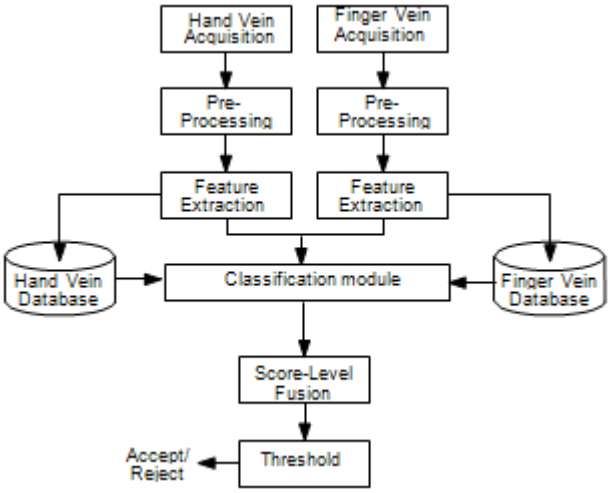

Fig. 12. Overview of the proposed method.

is presented by the following equation:

$$Nor = \frac{s-min}{max-min} \quad (11)$$

where [*min* and *max*] correspond respectively to the maximum and minimum scores for the print *S* (finger or hand vein)

obtained by the proposed system. Then, a combining score is processed as:

$$S = \frac{1}{N}\sum_{i}^{N} S_i \quad (12)$$

where *N* is the number of output matched scores. Finally, in the decision step the output matching scores *S* are evaluated to decide whether the samples of individuals as genuine or as imposters.

IV. EXPERIMENTS RESULTS

To evaluate the performance of our biometric system, we use the EER, FAR, FRR metrics and the Receiver Operating Characteristic (ROC) curve. This latter shows the representation of True Positive Rate (TPR) against the False Positive Rate (FPR). The Area Under the ROC Curve (AUC) is also a metric to evaluate the performance of our biometric system. The value of AUC will satisfies this inequality:

$$0.5 \leq AUC \leq 1 \quad (13)$$

Accordingly, if the AUC is close to area of unit square, the system presents a high security.

Experimental results show that the proposed multimodal biometric system gives a higher performance compared by unimodal biometric system (see Fig. 13).

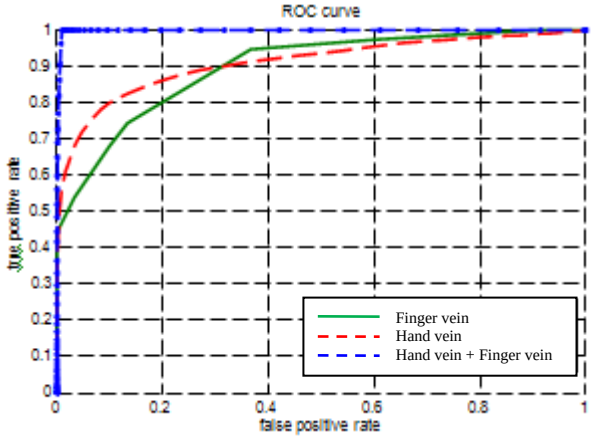

Fig. 13. Receiver Operating Characteristic (ROC) curve showing the performance when sum rule is used to combine the matching scores of hand vein and finger vein.

In Table II, we illustrate the experimental results of both algorithms of identification based on fusion of finger vein and hand vein modalities.

TABLE II
Performance Evaluation for Recognition Based on Hand Vein, Finger Vein and Fusion.

Trait	AUC	FAR	FRR	EER
Hand vein	0.87	1	1.41	1.1
Finger vein	0.89	1.14	1.56	1.2
Finger vein + Hand vein	0.98	0	1	0.004

In our proposed system, we combine two biological characteristics (hand vein + finger vein) and the result has increased performance of the biometric system.

TABLE III
Performance of our proposed System Based UPON Five Factors (P1=Universality, P2=Distinctiveness, P3=permanence, P4=Collectability, P5=Accessibility, H=High, M=Medium)

Biometric traits	P1	P2	P3	P4	P5
Hand vein	M	H	M	M	H
Finger vein	M	H	M	M	H
Fusion	H	H	H	H	H

V. CONCLUSION

In this paper, a new multimodal biometric system based on hand vein and finger vein has been investigated. Score level fusion for hand vein and finger vein attributes is processed. Experimental results clearly show that the proposed multimodal biometric process offers very good results when compared to the corresponding unimodal biometric system. Future work will focus on performing more experiments on a larger database that presents different acquired print of the same individual.

REFERENCES

[1] C. A. Vinodh, "Extracting and enhancing the core area in fingerprint images," *International Journal of Computer Science and Network Security*, vol. 7, no. 11, pp. 16–20, 2007.

[2] A. D. Masmoudi and D. S. Masmoudi, "Implementation of a fingerprint recognition system using lbp descriptor," *Journal of Testing and Evaluation*, vol. 38, no. 3, 2010.

[3] X. Pan and Q.-Q. Ruan, "Encoding local image patterns using riesz transforms: With applications to palmprint and finger-knuckle-print recognition,"*Image and Vision Computing*, pp. 1261–1268, 2008.

[4] T. Connie, A. T. B. Jin, M. G. K. Ong, and D. N. C. Ling, "An automated palmprint recognition system," *Image and Vision Computing*, pp. 501–515, 2005.

[5] T. Ahonen, A. Hadid, and M. Piesetikainen, "Face description with local binary patterns:application to face recognition," *IEEE Transactions on Pattern Analysis and Machine Intelligence*, pp. 2073–2041, 2006.

[6] L. Zhang and H. Li, "Encoding local image patterns using riesz transforms with applications to palmprint and finger knuckle print recognition," *Image and Vision Computing*, pp. 1043–1051, 2012.

[7] X.-Y. Jing, S. Li, W.-Q. Li, Y.-F. Yao, C. Lan, J.-S. Lu, and J.-Y. Yang, "Palmprint and face multi-modal biometric recognition based on sda-gsvd and its kernelization," *Sensors*, pp. 5551–5571, 2012.

[8] G. Park and S. Kim, "Hand biometric recognition based on fused hand geometry and vascular patterns," *Sensors*, pp. 2895–2910, 2013.

[9] R. B. Trabelsi, I. K. Kallel, and D. S. Masmoudi, "Person identification based on a new multimodal biometric system," *Transaction On Systems, Signals and Devices*, vol. 7, no. 3, pp. 273–289, 2012.

[10] A. Kumar, D. C. M. Wong, H. C. Shen, and A. K. Jain, "Personal verification using palmprint and hand geometry biometric," *Lecture Notes In Computer Science*, pp. 668–678, 2003.

[11] A. Kumar and K. Prathyusha, "Personal authentication using hand vein triangulation and knuckle shape," *IEEE Transaction on Image Process*, vol. 18, no. 9, pp. 2127–2136, 2009.

[12] B. Kang and K. Park, "Multimodal biometric method based on vein and geometry of a single finger," *Computer Vision, IET*, vol. 4, no. 3, pp. 209 – 217, 2010.

[13] Sdumla-hmt database. [Online]. Available: mla.sdu.edu.cn/sdumla-hmt.html? [14] Bosphorus database. [Online]. Available: bosphorus.ee.boun.edu.tr/hand/

[14] W. Lee, V. Alchanatis, C. Yang, M. Hirafuji, D. Moshou, and C. Lif, "Sensing technologies for precision specialty crop production," *Computers and Electronics in Agriculture*, vol. 74, no. 1, pp. 2–33, 2010.

[15] C. G. Homer, C. L. Aldridge, D. K. Meyer, and S. J. Schell, "Multi-scale remote sensing sagebrush characterization with regression trees over wyoming, usa: Laying a foundation for monitoring," *International Journal of Applied Earth Observation and Geoinformation*, vol. 14, no. 1, pp. 233–244, 2012.

[16] Y. Zhao, D. G. Nicolas, and E. Petriu, "Applying contrast-limited adaptive histogram equalization and integral projection for facial feature enhancement and detection," in *Instrumentation and Measurement Technology Conference (I2MTC), IEEE*, 2010, pp. 861–866.

[17] T. Ojala, M. Pietikinen, and T. Menp, "Multiresolution gray-scale and rotation invariant texture classification with local binary patterns," *IEEE Transaction on Pattern Analysis and Machine Intelligence*, vol. 24, pp. 971–987, 2002.

[18] S. Chaudhuri, S. Chatterjee, N. Katz, M. Nelson, and M. Goldbaum, "Detection of blood vessels in retinal images using two-dimensional matched filters," *IEEE Transaction on Medical Imaging*, vol. 8, no. 3, pp. 263–269, 1989.